

Contents lists available at ScienceDirect

Journal of Mathematical Analysis and Applications



journal homepage: www.elsevier.com/locate/jmaa

Regular Articles

The Buffon's needle problem for random planar disk-like Cantor sets

ABSTRACT



Dimitris Vardakis*, Alexander Volberg¹

Michigan State University, United States of America

ARTICLE INFO

Article history: Received 1 February 2023 Available online 26 July 2023 Submitted by L. Olsen

Keywords: Favard length Buffon needle Hausdorff measure Random Cantor sets We consider a model of randomness for self-similar Cantor sets of finite and positive 1-Hausdorff measure. We find the sharp rate of decay of the probability that a Buffon needle lands δ -close to a Cantor set of this particular randomness. Two quite different models of randomness for Cantor sets, by Peres and Solomyak, and by Shiwen Zhang, appear to have the same order of decay for the Buffon needle probability: $\frac{c}{\log \frac{1}{\delta}}$. In this note, we prove the same rate of decay for a third model of randomness, which asserts a vague feeling that any "reasonable" random Cantor set of positive and finite length will have Favard length of order $\frac{c}{\log \frac{1}{\delta}}$ for its δ -neighbourhood. The estimate from below was obtained long ago by Mattila.

© 2023 Elsevier Inc. All rights reserved.

Contents

1.	Introduction	2
2.	Cantor disks	3
	2.1. The \mathcal{D} operators	5
3.	Favard length	6
	Statement and use of the main lemma	
5.	Proving the main lemma	8
	5.1. Key observations	9
	5.2. The estimates	9
6.	Comparison with [12] and [11]	13
Ackno	owledgments	14
	ences	
Furth	er reading	15

^{*} Corresponding author.

E-mail addresses: jimvardakis@gmail.com (D. Vardakis), volberg@msu.edu (A. Volberg).

 $^{^{1}\,}$ AV is supported by NSF grants DMS 1900286 and DMS 2154402.

1. Introduction

Let E be a subset of the unit disk, \mathbb{D} . The Buffon needle problem wants to determine the probability with which a random needle or line intersects E provided that it already intersects the unit disk. At the same time, let l_{θ} be the line passing through the origin and forming angle θ with the horizontal axis. The Favard length of E is the average length of the projection of E onto l_{θ} when averaging over all angles θ . It turns out these two quantities are proportional.

Now, consider the following picture: let us have L many $(L \geq 3)$ disjoint closed disks (D_1, \ldots, D_L) of diameter 1/L and strictly inside \mathbb{D} . These are disks of the first generation. Consider also a piecewise affine map $f = (f_1, \ldots, f_L)$ from those disks onto \mathbb{D} . Then, $f^{-1}(\mathbb{D}) = D_1 \cup \cdots \cup D_L$. Furthermore, $f^{-1}(D_1 \cup \cdots \cup D_L)$ it consists of L^2 disks (groups of L many disks in each D_i); we call those disks of the second generation. We can iterate this procedure: denoting by U_n the union of disks of the n-th generation, where $U_1 := D_1 \cup \cdots \cup D_L$, we form the self-similar Cantor set $\mathcal{K} = \bigcap_{n=1}^{\infty} U_n$. This has positive and finite 1-dimensional Hausdorff measure; thus it is completely unrectifiable in the sense of Besicovitch [8]; and thus its Favard length is zero [8].

Of course, the disks can be replaced by other shapes. For example, U_1 can consist of L disjoint squares with side-length 1/L inside the unit square $[0,1]^2$ (where the word "strictly" can be omitted but "disjoint" cannot). One of such Cantor sets is a rather "famous", namely the 1/4-corner Cantor set, $\mathcal{K}_{1/4}$ (see [7]).

The L^{-n} -neighbourhood of such sets is roughly U_n , and therefore its Favard length

$$Fav(U_n) \to 0$$
, as $n \to \infty$.

But what is $Fav(U_n)$, or what is the speed with which $Fav(U_n)$ decreases? Nobody knows exactly, but there has been considerable interest in recent years. It is now clear that the answer may depend on several factors; the magnitude of L; the geometry of U_1 ; the subtle algebraic and number theoretic properties of a certain trigonometric sum built by the centres of the disks of the first generation. See [2–4,6,10] and the survey paper [5].

For the 1/4-corner Cantor set $\mathcal{K}_{1/4}$ in particular, the best known estimate from above for its 4^{-n} -neighbourhood is

$$\operatorname{Fav}(N_{4^{-n}}(\mathcal{K}_{1/4})) \leq \frac{C_{\varepsilon}}{n^{\frac{1}{6}-\varepsilon}}, \quad \forall \varepsilon > 0,$$

for all large n. We suspect that this estimate can be improved to

$$\operatorname{Fav}(N_{4^{-n}}(\mathcal{K}_{1/4})) \le \frac{C_{\varepsilon}}{n^{1+\varepsilon}}, \quad \forall \varepsilon > 0,$$

but at this moment this is only a conjecture.

On the other hand, there is a universal estimate from below obtained in [9] for every self-similar Cantor set constructed as above:

$$\operatorname{Fav}(N_{4^{-n}}(\mathcal{K})) \ge \frac{c}{n}.\tag{1.1}$$

For any concrete set, this bound from below could be improved. In fact, it is proven in [1] that for the same 1/4-corner Cantor set $\mathcal{K}_{1/4}$

$$\operatorname{Fav}(N_{4^{-n}}(\mathcal{K}_{1/4})) \ge \frac{c \log n}{n}.$$

For random Cantor sets the situation should be simpler. With large probability, Mattila's lower estimate (1.1) is met by *the same* estimate from above (with a different constant). The problem is that in general there can be many different models of randomness.

In this note, we are interested in an analogue of the random Cantor set appearing in [11] and in [12]. In our case, this will come from the random Cantor disks constructed below at Section 2. The model of randomness presented here is somewhat different from the ones in the above two papers, but it amazingly exhibits the same behaviour, as we'll see below in our main Theorem 1, which we contrast with [11, Theorem 2.2] and [12, Theorem 1].

In particular, we prove an analogue of [12, Theorem 1]. Unfortunately, the randomness of the disk model we study here is not equivalent to that of the random (square) Cantor set $\mathcal{R} = \bigcap_{n=0}^{\infty} \mathcal{R}_n$ from [11], but it is nonetheless closer compared to the one constructed in [12]. The essential difference between [12] and our consideration are the angles $\omega_n^1, \omega_n^2, \ldots, \omega_n^{4^{n-1}}$, which are here allowed to be distinct and independent whereas in [12] are all equal. So, our model is a little "more random" than the random Cantor sets of Zhang in [12].

We introduce our notations—some borrowed from [12]—in the next Section 2. The problem of interest, namely the *Favard length* of a random planar disk-like Cantor set, is explained in Section 3. Our results and their proofs are postponed to Sections 4 and 5. In Section 6, we compare the differences and difficulties between our work and that of Peres and Solomyak's and Zhang's.

2. Cantor disks

Our work will be heavy on notation; without any ado let us introduce our basic "vocabulary".

The letter n will stand for a (large) positive integer.

The letter ω will be used to denote angles with values inside the interval $[0, \frac{\pi}{2}]$. Now, let us consider a word of length n made of the alphabet of angles in $[0, \frac{\pi}{2}]$, i.e. a word of the form $\omega_1\omega_2\cdots\omega_n$. The subscript in ω_k denotes the position of the angle ω_k within such a word of length n. We refer to the position of an angle within a word as the *depth* of that angle.

Our operators, which we will introduce below, are such that every choice of an angle, say, ω_1 necessitates four different independent choices for the angle ω_2 ; every choice of the angle ω_2 necessitates four different independent choices for the angle ω_3 ; and so on up until depth n where we will have 4^{n-1} different angles ω_n . In order to differentiate between all those, for each $j_k = 1, 2, \ldots, 4^{k-1}$ we write $\omega_k^{j_k}$ for the j_k -th choice of an angle ω_k at depth k. Notice there are 4^{k-1} such choices. Therefore, a typical word from our alphabet of angles looks as follows, where we note that $\omega_k^{j_k} \in [0, \frac{\pi}{2}]$:

At certain instances, we need to consider cumulatively all angles of a certain depth; given a collection of words of length n, for each k = 1, 2, ..., n let ω'_k be the collection of all 4^{k-1} many angles at depth k, that is

$$\omega_k' = (\omega_k^1, \dots, \omega_k^{4^{k-1}}).$$

With this notation, we may use the symbols ω_1 , $\omega_1^{j_1}$, ω_1^1 , and ω_1' interchangeably as these all refer to the same single angle.

All the above give to our angles the structure of a rooted tree of height n with root ω_1 and such that each parent has four children as in Fig. 1. The vertexes have values in $[0, \frac{\pi}{2}]$, and are independent from each

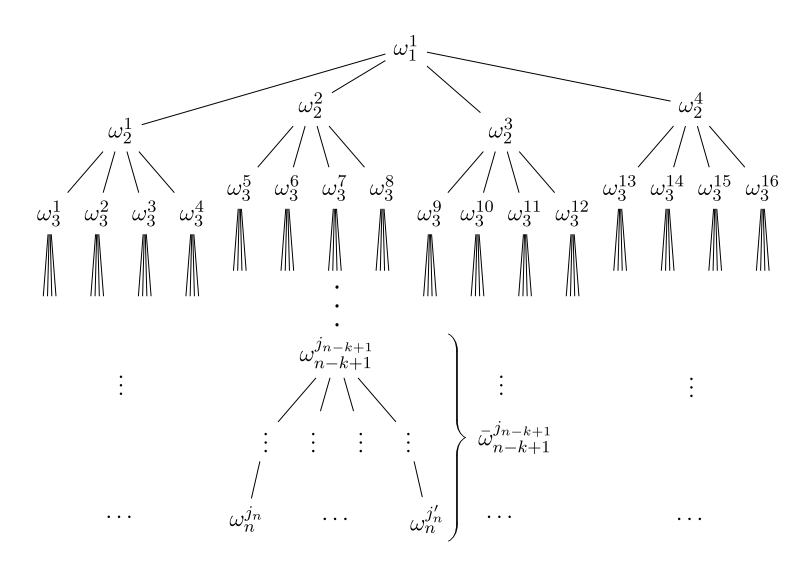


Fig. 1. The *n*-tree of angles with root ω_1^1 , all angles of depth 1 to 3, and the subtree $\bar{\omega}_{n-k+1}^{j_{n-k+1}}$ of height k with root $\omega_{n-k+1}^{j_{n-k+1}}$ at depth n-k+1. All angles are enumerated. (The exact values of j_n and j'_n depend on j_{n-k+1} .)

other and from their predecessors and ancestors. This tree we denote by $\omega_1' \cdots \omega_n'$; the trimmed tree with root ω_1 and height k we denote as $\omega_1' \cdots \omega_k'$ (for any $k = 1, 2, \ldots, n$). For the subtree of height n - k + 1 with root $\omega_k^{j_k}$, which reaches up to the leaves (that is, from depth k till depth n with starting vertex $\omega_k^{j_k}$) we write $\bar{\omega}_k^{j_k}$. Later on, we will be working with rooted subtrees of the form $\bar{\omega}_{n-k+1}^{j_{n-k+1}}$. To reiterate, $\bar{\omega}_{n-k+1}^{j_{n-k+1}}$ consists of the angle $\omega_{n-k+1}^{j_{n-k+1}}$ (as its root) along with all the angles from depth n-k+1 till depth n (which have $\omega_{n-k+1}^{j_{n-k+1}}$ as an ancestor). This has height k. Alternatively, $\bar{\omega}_{n-k+1}^{j_{n-k+1}}$ is the collection of all the words (from our alphabet of angles) which have depth (i.e. length) k and the first letter is $\omega_{n-k+1}^{j_{n-k+1}}$. There are 4^{n-k} such words.

Next, we will need to introduce certain operators and sets. The main objects of interest will be the operators \mathcal{D}_k $(k=0,1,\ldots,n)$ which will act on trees of angles of depth k. To understand these we need some auxiliary constructions first.

For any angle ω and for $\alpha = 0, 1, 2, 3$ consider the transformations

$$T_{\alpha}^{\omega}(z) = \frac{1}{4}z + \frac{3}{4}e^{(\alpha\frac{\pi}{2} - \omega)i}$$
 (2.1)

where z is any number on the complex plane \mathbb{C} . Observe that if \mathbb{D} is the unit disk, $T_0^0(\mathbb{D})$, $T_1^0(\mathbb{D})$, $T_2^0(\mathbb{D})$, and $T_3^0(\mathbb{D})$ are disks of radius 1/4 centred respectively at (3/4,0), (0,3/4), (-3/4,0), and (0, -3/4). Introducing an angle ω in $T_{\alpha}^{\omega}(\mathbb{D})$, rotates (about (0,0)) the aforementioned disks by angle ω in the clockwise direction. Moreover, given an angle $\omega_k^{j_k}$ from depth k let $\Omega_k^{j_k}$ be the set

$$\Omega_k^{j_k} = \bigcup_{\alpha=0}^3 \frac{1}{4^{k-1}} T_{\alpha}^{\omega_k^{j_k}}(\mathbb{D}).$$

That is, $\Omega_k^{j_k}$ is a collection of four disks of radius 4^{-k} with centres $(0, \pm 3/4^k)$ and $(\pm 3/4^k, 0)$ rotated clockwise by $\omega_k^{j_k}$. An example of Ω_2^1 appears on Fig. 2.

We also give an enumeration to all the disks for all depths. We number the disks of $\Omega_k^{j_k}$ so that $\frac{1}{4^{k-1}}T_{\alpha}^{\omega_k^{j_k}}(\mathbb{D})$ is the $(4j_k-3+\alpha)$ -th disk at depth k. We call this the k-depth enumeration (of the disks lying at depth k). Illustratively, we note $\frac{1}{4^{k-1}}T_0^{\omega_k^{l}}(\mathbb{D})$, $\frac{1}{4^{k-1}}T_1^{\omega_k^{l}}(\mathbb{D})$, $\frac{1}{4^{k-1}}T_0^{\omega_k^{k}^{l-1}}(\mathbb{D})$, $\frac{1}{4^{k-1}}T_3^{\omega_k^{k-1}}(\mathbb{D})$ are the 1st,

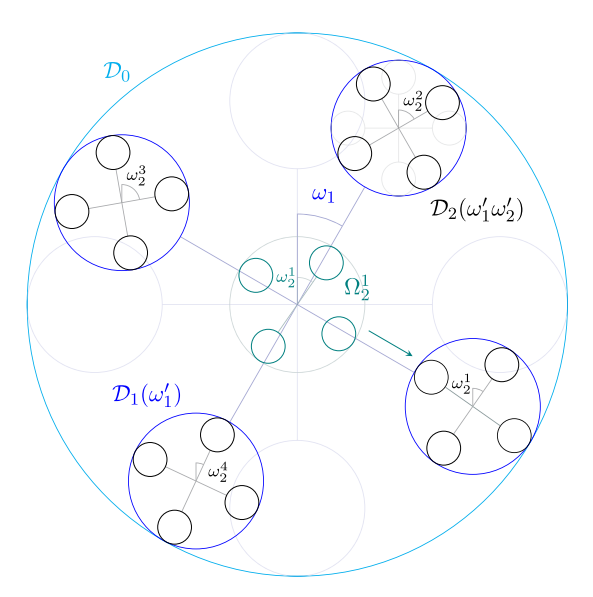


Fig. 2. The collections \mathcal{D}_0 , $\mathcal{D}_1(\omega_1')$, $\mathcal{D}_2(\omega_1'\omega_2')$ and Ω_2^1 .

2nd, $(4^k - 3)$ -th, 4^k -th disks of depth k. We retain this enumeration as we translate these disks at different positions on the plane. This will be useful to track down each disk at each step so that our subsequent constructions make better sense.

2.1. The \mathcal{D} operators

Now, we are ready to introduce our main protagonists. The operator \mathcal{D}_k acts on the collection of trees (of angles) of height k and for each such tree outputs a certain collection of 4^k disks of radius 4^{-k} . We define these inductively below.

To begin with, set $\mathcal{D}_0 = \mathbb{D}$ to be the unit disk.

Next, we define \mathcal{D}_1 by

$$\mathcal{D}_1(\omega_1') = \Omega_1^1 = \bigcup_{\alpha=0}^3 T_{\alpha}^{\omega_1^1}(\mathcal{D}_0), \tag{2.2}$$

that is, $\mathcal{D}_1(\omega_1')$ consists of four disks of radius 1/4 centred at $(0, \pm 3/4)$ and $(\pm 3/4, 0)$ rotated clockwise by ω_1 . Recall these disks are enumerated as in Ω_1^1 above.

For the operator \mathcal{D}_2 , consider a tree of height 2, $\omega_1'\omega_2'$, which consists of the angles ω_1^1 , and $\omega_2^1, \omega_2^2, \omega_2^3, \omega_2^4$. Then, we define $\mathcal{D}_2(\omega_1'\omega_2')$ to be the collection of disks constructed as follows: Replace the 1st, 2nd, 3rd and 4th disk of $\mathcal{D}_1(\omega_1')$ respectively by Ω_2^1 , Ω_2^2 , Ω_2^3 and Ω_2^4 . By "replacing" we mean the translation of Ω_2^j in such a way that (0,0) is translated to the centre of the j-th disk of $\mathcal{D}_1(\omega_1')$.

Consequently, $\mathcal{D}_2(\omega_1'\omega_2')$ consists of 4^2 disks of radius 4^{-2} translated appropriately so that each $\Omega_2^{j_2}$ (which is a collection of four disks) replaces one of the disks from $\mathcal{D}_1(\omega_1')$. For example, the set Ω_2^1 is in fact a subset of the 1st disk of $\mathcal{D}_1(\omega_1')$; actually $\mathcal{D}_2(\omega_1'\omega_2') \subset \mathcal{D}_1(\omega_1')$. Again, the disks comprising $\mathcal{D}_2(\omega_1'\omega_2')$ are enumerated to match Ω_2^1 , Ω_2^2 , Ω_2^3 and Ω_2^4 as we described above. Also see Fig. 2.

Continuing inductively, the operator \mathcal{D}_k acts on the tree $\omega_1' \cdots \omega_k'$ in this manner: Consider the collection $\mathcal{D}_{k-1}(\omega_1' \cdots \omega_{k-1}')$. These are 4^{k-1} many (enumerated) disks. Replace the 1st of them by Ω_k^1 , the 2nd of them by Ω_k^2 , etc., until every disk of $\mathcal{D}_{k-1}(\omega_1' \cdots \omega_{k-1}')$ has been replaced by four smaller ones. This replacement is done so that (0,0), as the "centre" of Ω_k^j , is translated to the centre of the j-th disk of $\mathcal{D}_{k-1}(\omega_1' \cdots \omega_{k-1}')$. That is, we substitute the j-th disk (from depth k-1) with the (4j-3)-, (4j-2)-, (4j-1)-, and 4j-th

disks of depth k. The resulting collection, which has 4^k many disks of radius 4^{-k} , is $\mathcal{D}_k(\omega_1' \dots \omega_k')$. It holds that $\mathcal{D}_k(\omega_1' \dots \omega_k') \subset \mathcal{D}_{k-1}(\omega_1' \dots \omega_{k-1}')$.

In the present work, we will study the collection of disks $\mathcal{D}_n(\omega_1'\cdots\omega_n')$ where the angles $\omega_k^{j_k}$ (for $j_k=1,\ldots,4^{k-1}$ and all $k=1,2,\ldots,n$) of the tree $\omega_1'\cdots\omega_n'$ are chosen randomly with uniform and independent distributions on the interval $[0,\frac{\pi}{2}]$.

Let us describe this picture once more before moving on further. The set $\mathcal{D}_n(\omega_1'\cdots\omega_n')$ consists of 4^n disks of radius 4^{-n} . These can be separated into 4^{n-1} groups of four, which are copies of

$$\Omega_n^{j_n} = \bigcup_{\alpha=0}^3 \frac{1}{4^{n-1}} T_\alpha^{\omega_n^{j_n}} (\mathcal{D}_0)$$

translated appropriately within the unit disk so that the "centre" of $\Omega_n^{j_n}$ is placed at the centre of the j_n -th disk of $\mathcal{D}_{n-1}(\omega_1'\ldots\omega_{n-1}')$ for $j_n=1,2,\ldots,4^{n-1}$. That is, each of the 4^{n-1} many disks at depth n-1 of radius $4^{-(n-1)}$ is replaced by four smaller ones of radius 4^{-n} . Fig. 2 depicts $\mathcal{D}_n(\omega_1'\cdots\omega_n')$ for n=0,1,2.

3. Favard length

Recall the Favard length of a planar set $E \subset \mathbb{C}$ is the integral

$$\operatorname{Fav}(E) = \frac{1}{\pi} \int_{0}^{\pi} |\operatorname{proj}_{\theta} E| \, d\theta$$

where $\operatorname{proj}_{\theta} E$ is the projection of E onto the line with slope $\tan \theta$ passing through the origin, and |A| is the (1-dimensional) Lebesgue measure of A.

Now, consider an infinite tree of angles from $[0, \frac{\pi}{2}]$ with root ω_1 and four branches at each vertex, and let \mathcal{D} be the limit set

$$\mathcal{D} = \bigcap_{n=0}^{\infty} \mathcal{D}_n(\omega_1' \cdots \omega_n').$$

Notice that by construction, \mathcal{D} a purely unrectifiable planar set. As such, $\operatorname{Fav}(\mathcal{D}) = 0$ and by dominated convergence $\operatorname{Fav}(\mathcal{D}_n(\omega_1' \cdots \omega_n')) \to 0$ while $n \to \infty$. In fact, if the angles are randomly chosen uniformly and independently over $[0, \frac{\pi}{2}]$, by dominated convergence and Fubini $\mathbb{E}[\operatorname{Fav}(\mathcal{D})] = 0$ and $\mathbb{E}[\operatorname{Fav}(\mathcal{D}_n(\omega_1' \cdots \omega_n'))] \to 0$ as $n \to \infty$, where the expectation is taken over all such angles.

The question arises as to the rate with which $\mathbb{E}[\operatorname{Fav}(\mathcal{D}_n(\omega_1'\cdots\omega_n'))]$ goes to 0. This we answer in the following theorem:

Theorem 1. Let $n \in \mathbb{N}$ and consider a tree of angles of height n with each vertex having four branches. Suppose that the angles $\omega_k^{j_k}$ (for all $j_k = 1, 2, ..., 4^{k-1}$ and all k = 1, 2, ..., n) are chosen randomly with uniform and independent distributions on the interval $[0, \frac{\pi}{2}]$. Also set $\omega_k' = (\omega_k^1, \omega_k^2, ..., \omega_k^{4^{k-1}})$ for each k = 1, 2, ..., n. Then, there exists a constant c > 0 such that for any $\theta \in [0, \frac{\pi}{2}]$ it holds that

$$\mathbb{E}_{\omega'_1 \cdots \omega'_n} \left| \operatorname{proj}_{\theta} \mathcal{D}_n(\omega'_1 \cdots \omega'_n) \right| \le \frac{c}{n} \qquad \forall n \in \mathbb{N}.$$
(3.1)

Consequently,

$$\mathbb{E}_{\omega_1' \cdots \omega_n'} [\operatorname{Fav}(\mathcal{D}_n(\omega_1' \cdots \omega_n'))] \le \frac{c}{n} \qquad \forall n \in \mathbb{N}$$
(3.2)

and also

$$\liminf_{n \to \infty} n \operatorname{Fav}(\mathcal{D}_n(\omega_1' \cdots \omega_n')) < \infty \qquad \forall n \in \mathbb{N} \ almost \ surely.$$
 (3.3)

Clearly, (3.3) follows from (3.2) by an immediate application of Fatou's lemma, whereas (3.2) follows from (3.1) through Fubini.

4. Statement and use of the main lemma

The present and the following sections are dedicated to the proof of (3.1). Towards this goal, we need to introduce Lemma 2 below, which describes the decay of the average projection when transitioning from depth k to depth k+1. The main difficulty will come from obtaining the square factor appearing in (4.1), which emanates from the naturally occurring overlap of the projections.

From now on, suppose we are given a tree of angles of height n with four branches at each vertex where the angles are uniformly and independently distributed random variables on the interval $[0, \frac{\pi}{2}]$. Recall that given such a tree $\bar{\omega}_{n-k+1}^{j_{n-k+1}}$ is the subtree of height k with the vertex $\omega_{n-k+1}^{j_{n-k+1}}$ as its root. Observe that $\bar{\omega}_1^{j_1} = \omega_1' \cdots \omega_n'$ is the full tree whilst $\bar{\omega}_n^{j_n} = \omega_n^{j_n}$ $(j_n = 1, 2, \dots, 4^{n-1})$ are its leaves, i.e. trees of height 1.

For any $\theta \in [0, \frac{\pi}{2}]$ and all $k = 1, 2, \dots, n$, define the following quantities

$$D_{1}^{j_{n}} = \mathbb{E}_{\bar{\omega}_{n}^{j_{n}}} \left| \operatorname{proj}_{\theta} \mathcal{D}_{1}(\bar{\omega}_{n}^{j_{n}}) \right|, \qquad j_{n} = 1, 2, \dots, 4^{n-1}$$

$$D_{k}^{j_{n-k+1}} = \mathbb{E}_{\bar{\omega}_{n-k+1}^{j_{n-k+1}}} \left| \operatorname{proj}_{\theta} \mathcal{D}_{k}(\bar{\omega}_{n-k+1}^{j_{n-k+1}}) \right|, \qquad j_{n-k+1} = 1, 2, \dots, 4^{n-k}$$

$$D_{n}^{j_{1}} = D_{n}^{1} = \mathbb{E}_{\bar{\omega}_{1}^{j_{1}}} \left| \operatorname{proj}_{\theta} \mathcal{D}_{n}(\bar{\omega}_{1}^{j_{1}}) \right|, \qquad j_{1} = 1.$$

Notice that, because we are averaging over the independent and identically distributed $\omega_k^{j_k}$,

$$D_k^1 = D_k^2 = \dots = D_k^{4^{n-k}}$$
 for any $k = 1, 2, \dots, n$.

Therefore, it suffices to work with D_k^1 ; the rest should be identical. Also, note that

$$D_n^1 = \mathbb{E}_{\omega_1' \cdots \omega_n'} \left[\operatorname{proj}_{\theta} \mathcal{D}_n(\omega_1' \cdots \omega_n') \right].$$

Now, we are ready to state a simple but important lemma. Also, see [12, Lemma 2.1].

Lemma 2. With notation as above, if $\omega_k^{j_k}$ are uniformly and independently distributed random variables on $[0, \frac{\pi}{2}]$, there exists a constant $c \geq 4$ such that for any $n \in \mathbb{N}$ (and any $\theta \in [0, \frac{\pi}{2}]$)

$$D_{k+1}^1 \le D_k^1 - c^{-1}(D_k^1)^2$$
 for all $k = 1, \dots, n-1$. (4.1)

In our computations later, we will have that $c = 12\sqrt{2}$. But this is possibly not sharp.

Provided this holds true we can give a very compact proof of Theorem 1 using induction:

Proof of Theorem 1. Let c be as in Lemma 2 and note that $D_2^1 \le D_1^1 < 2 \le \frac{c}{2}$. Also, $D_1^1 < c$.

Next, assume $D_k^1 < \frac{c}{k}$ for some $2 \le k \le n-1$. From Lemma 2, and by the monotonicity of the function $x - x^2/c$ in $[0, \frac{c}{2}]$, we see that

$$D_{k+1}^1 \le D_k^1 - c^{-1}(D_k^1)^2 < \frac{c}{k} - \frac{c}{k^2} = c\frac{k-1}{k^2} < \frac{c}{k+1}.$$

Therefore, $D_k^1 < \frac{c}{k}$ holds for all for $1 \le k \le n-1$ and thus for k=n we get

$$\mathbb{E}_{\omega_1' \cdots \omega_n'} \left| \operatorname{proj}_{\theta} \mathcal{D}_n(\omega_1' \cdots \omega_n') \right| = D_n^1 < \frac{c}{n}.$$

This is (3.1). Equation (3.2) follows after integrating with respect to θ , and (3.3) after applying Fatou's Lemma. \Box

5. Proving the main lemma

Whatever follows is dedicated to the proof of (4.1).

First, we rewrite the length of the projection of a set in more convenient way. Let l_{θ} and l_{θ}^{\perp} be two lines through the origin so that l_{θ} forms an angle θ with the horizontal axis and l_{θ}^{\perp} is perpendicular to l_{θ} . Also, let **n** be the unit normal vector of l_{θ}^{\perp} . The length of the projection of a planar set $E \subset \mathbb{C}$ onto the line l_{θ} can be written as

$$|\operatorname{proj}_{\theta} E| = \left| \{ t \in \mathbb{R} : (l_{\theta}^{\perp} + t\mathbf{n}) \cap E \neq \emptyset \} \right| = \int_{(l_{\theta}^{\perp} + t\mathbf{n}) \cap E \neq \emptyset} dt.$$
 (5.1)

For brevity, we denote the line $l_{\theta}^{\perp} + t\mathbf{n}$ by $l_{\theta}^{\perp}(t)$ where $t \in \mathbb{R}$. Additionally, because of the symmetry of our considerations, we can assume without loss of generality that $\theta = 0$ —as we will average over all θ at the end. So, we can simply omit writing θ altogether from now on.

The idea behind Lemma 2 is to look at the collection $\mathcal{D}_n(\omega_1'\cdots\omega_n')$ at depth n but "zoomed in" so that it looks like depth 1. Then, we go one level up and look at the disks of depth n-1 and n zooming in enough so that they to look like depth 2; and so forth. If we rewrite the projections in the form of (5.1), the average overlap at each level is of at least a square factor compared to the total average projection of the level above.

This last comparison is paramount to the proof. It will follow from the fact that the disks in our constructions never get too close to one another. In fact, this observation is not true in the case of the random square Cantor sets, which is the reason why we cannot directly apply the arguments here to the setting of [11].

Let us proceed with the proof of (4.1).

Fix some k = 1, 2, ..., n and recall that by construction (eq. (2.2))

$$\mathcal{D}_1(\omega_{n-k+1}^1) = \bigcup_{\alpha=0}^3 T_{\alpha}^{\omega_{n-k+1}^1}(\mathcal{D}_0).$$

This means that each disk from the collection $\mathcal{D}_k(\bar{\omega}_{n-k+1}^1)$ lies inside one of the above four disks, and therefore we can separate $\mathcal{D}_k(\bar{\omega}_{n-k+1}^1)$ into four groups of disks depending on their positioning at depth 1. More precisely, for each $\alpha = 0, 1, 2, 3$ define $\mathcal{T}_{\alpha}^k(\bar{\omega}_{n-k+1}^1)$ as

$$\mathcal{T}_{\alpha}^{k}(\bar{\omega}_{n-k+1}^{1}) = \mathcal{T}_{\alpha}^{\omega_{n-k+1}^{1}}(\mathcal{D}_{0}) \cap \mathcal{D}_{k}(\bar{\omega}_{n-k+1}^{1}). \tag{5.2}$$

That is, the set $\mathcal{T}_{\alpha}^{k}(\bar{\omega}_{n-k+1}^{1})$ consists of those disks of $\mathcal{D}_{k}(\bar{\omega}_{n-k+1}^{1})$ which lie inside the $\frac{1}{4}$ -radius disk $\mathcal{T}_{\alpha}^{\omega_{n-k+1}^{1}}(\mathcal{D}_{0})$ as in Fig. 3. We can think of $\mathcal{T}_{\alpha}^{k}(\bar{\omega}_{n-k+1}^{1})$ as the East, North, West, and South parts of $\mathcal{D}_{k}(\bar{\omega}_{n-k+1}^{1})$, respectively for $\alpha = 0, 1, 2, 3$. From this definition, it is also clear that

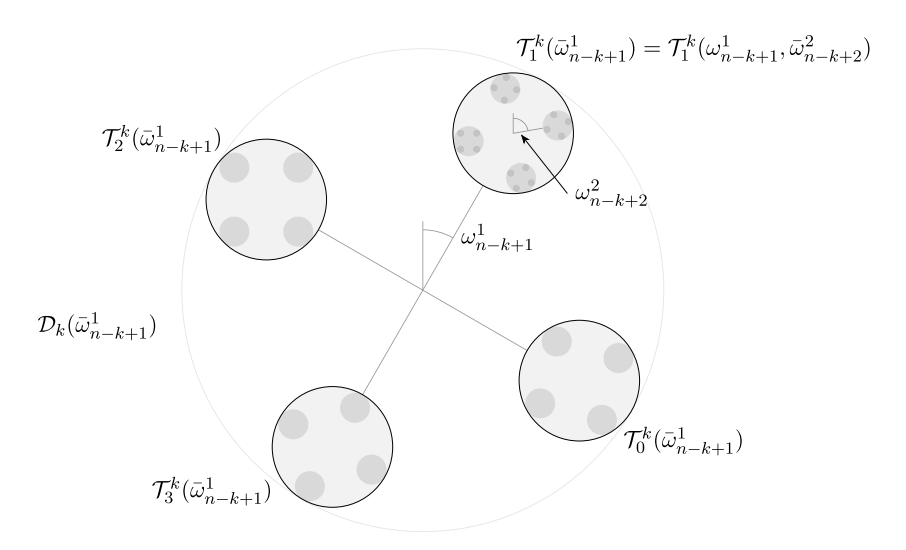


Fig. 3. The four groups of disks at depth k rotated by ω_{n-k+1}^1 , which make up $\mathcal{D}_k(\bar{\omega}_{n-k+1}^1)$.

$$\mathcal{D}_{k}(\bar{\omega}_{n-k+1}^{1}) = \bigcup_{\alpha=0}^{3} \mathcal{T}_{\alpha}^{k}(\bar{\omega}_{n-k+1}^{1}). \tag{5.3}$$

In fact, $\mathcal{T}_{\alpha}^{k}(\bar{\omega}_{n-k+1}^{1})$ depends only on the angle ω_{n-k+1}^{1} and the subtree $\bar{\omega}_{n-k+2}^{4\cdot 1-3+\alpha} = \bar{\omega}_{n-k+2}^{1+\alpha}$. (Recall our enumeration of the angles in Section 2.) Thus, we can write $\mathcal{T}_{\alpha}^{k}(\bar{\omega}_{n-k+1}^{1})$ as

$$\mathcal{T}_{\alpha}^{k}(\bar{\omega}_{n-k+1}^{1}) = \mathcal{T}_{\alpha}^{k}(\omega_{n-k+1}^{1}, \bar{\omega}_{n-k+2}^{1+\alpha}). \tag{5.4}$$

5.1. Key observations

There are two key observations regarding the sets $\mathcal{T}_{\alpha}^{k}(\bar{\omega}_{n-k+1}^{1})$. First, note that each point of the interval (-1,1) can be covered by at most two of the projections $\operatorname{proj} \mathcal{T}_{\alpha}^{\omega_{n-k+1}^{1}}(\mathcal{D}_{0})$ for different α 's. Since $\mathcal{T}_{\alpha}^{k}(\bar{\omega}_{n-k+1}^{1}) \subset \mathcal{T}_{\alpha}^{\omega_{n-k+1}^{1}}(\mathcal{D}_{0})$, the same holds true for $\operatorname{proj} \mathcal{T}_{\alpha}^{k}(\bar{\omega}_{n-k+1}^{1})$; the intersection $\bigcap_{\alpha} \operatorname{proj} \mathcal{T}_{\alpha}^{k}(\bar{\omega}_{n-k+1}^{1})$ is empty when the intersection is over more than two values of α .

Second, we can compare the average projections of $\mathcal{T}_{\alpha}^{k}(\bar{\omega}_{n-k+1}^{1}) = \mathcal{T}_{\alpha}^{k}(\omega_{n-k+1}^{1}, \bar{\omega}_{n-k+2}^{1+\alpha})$ and $\mathcal{D}_{k-1}(\bar{\omega}_{n-k+2}^{1+\alpha})$. Notice that both these collections consist of 4^{k-1} many disks, which in fact have the same n-depth enumerations. This means that they correspond to the same disks of the collection $\mathcal{D}_{n}(\omega_{1}'\cdots\omega_{n}')$. The difference is that the disks of the former are translated according to $\mathcal{D}_{1}(\omega_{n-k+1}^{1})$ and have radius 4^{-k} , whereas the ones of the latter have radius $4^{-(k-1)}$.

Consequently, $\mathcal{T}_{\alpha}^{k}(\bar{\omega}_{n-k+1}^{1})$ is a shifted copy of $\mathcal{D}_{k-1}(\bar{\omega}_{n-k+2}^{1+\alpha})$ dilated by a factor of 1/4. (See Fig. 4.) As such, the (average of the) projections of $\mathcal{T}_{\alpha}^{k}(\bar{\omega}_{n-k+1}^{1})$ and $\mathcal{D}_{k-1}(\bar{\omega}_{n-k+2}^{1+\alpha})$ should also differ by a factor of 1/4. In other words, for any $\alpha = 0, 1, 2, 3$ we have

$$\mathbb{E}_{\bar{\omega}_{n-k+1}^{1}} \left| \operatorname{proj} \mathcal{T}_{\alpha}^{k} (\bar{\omega}_{n-k+1}^{1}) \right| = \mathbb{E}_{\omega_{n-k+1}^{1}} \mathbb{E}_{\bar{\omega}_{n-k+2}^{1+\alpha}} \left| \operatorname{proj} \mathcal{T}_{\alpha}^{k} (\omega_{n-k+1}^{1}, \bar{\omega}_{n-k+2}^{1+\alpha}) \right| \\
= \frac{1}{4} \mathbb{E}_{\bar{\omega}_{n-k+2}^{1+\alpha}} \left| \operatorname{proj} \mathcal{D}_{k-1} (\bar{\omega}_{n-k+2}^{1+\alpha}) \right|.$$
(5.5)

5.2. The estimates

Utilising the above, we can now estimate D_k^1 in terms of D_{k-1}^1 .

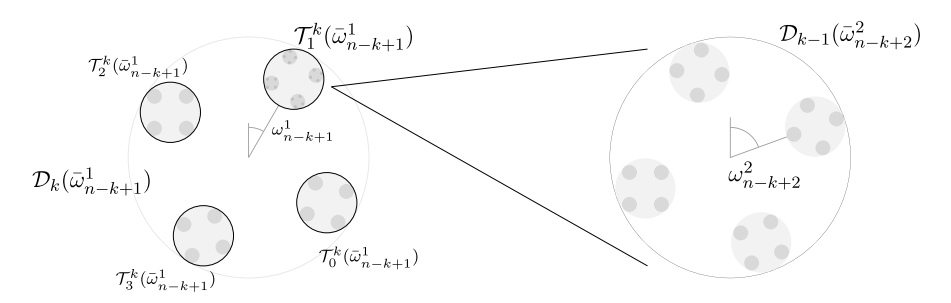


Fig. 4. Dilating $\mathcal{T}_1^k(\bar{\omega}_{n-k+1})$ by 4 gives a copy of $\mathcal{D}_{k-1}(\bar{\omega}_{n-k+2}^2)$.

For starters, note that from (5.3) we can write

$$\begin{split} D_k^1 &= \mathbb{E}_{\bar{\omega}_{n-k+1}^1} \left| \operatorname{proj} \mathcal{D}_k(\bar{\omega}_{n-k+1}^1) \right| \\ &= \mathbb{E}_{\bar{\omega}_{n-k+1}^1} \sum_{\alpha=0}^3 \left| \operatorname{proj} \mathcal{T}_{\alpha}^k(\bar{\omega}_{n-k+1}^1) \right| - \mathbb{E}_{\bar{\omega}_{n-k+1}^1} \sum_{\substack{\alpha,\beta=0 \\ \alpha \neq \beta}}^3 \left| \operatorname{proj} \mathcal{T}_{\alpha}^k(\bar{\omega}_{n-k+1}^1) \cap \operatorname{proj} \mathcal{T}_{\beta}^k(\bar{\omega}_{n-k+1}^1) \right| + \\ &+ \mathbb{E}_{\bar{\omega}_{n-k+1}^1} \sum_{\substack{\alpha,\beta,\gamma=0 \\ \alpha \neq \beta \neq \gamma \neq \alpha}}^3 \left| \operatorname{proj} \mathcal{T}_{\alpha}^k(\bar{\omega}_{n-k+1}^1) \cap \operatorname{proj} \mathcal{T}_{\beta}^k(\bar{\omega}_{n-k+1}^1) \cap \operatorname{proj} \mathcal{T}_{\gamma}^k(\bar{\omega}_{n-k+1}^1) \right| - \\ &- \mathbb{E}_{\bar{\omega}_{n-k+1}^1} \left| \operatorname{proj} \mathcal{T}_0^k(\bar{\omega}_{n-k+1}^1) \cap \operatorname{proj} \mathcal{T}_1^k(\bar{\omega}_{n-k+1}^1) \cap \operatorname{proj} \mathcal{T}_2^k(\bar{\omega}_{n-k+1}^1) \cap \operatorname{proj} \mathcal{T}_3^k(\bar{\omega}_{n-k+1}^1) \right|. \end{split}$$

The last two lines equal 0 from our first observation above (in Section 5.1). Furthermore, we can disregard all but one of the summands from the second sum to get an inequality:

$$D_k^1 \leq \mathbb{E}_{\bar{\omega}_{n-k+1}^1} \sum_{\alpha=0}^3 \left| \operatorname{proj} \mathcal{T}_{\alpha}^k(\bar{\omega}_{n-k+1}^1) \right| - \mathbb{E}_{\bar{\omega}_{n-k+1}^1} \left| \operatorname{proj} \mathcal{T}_0^k(\bar{\omega}_{n-k+1}^1) \cap \operatorname{proj} \mathcal{T}_1^k(\bar{\omega}_{n-k+1}^1) \right|. \tag{5.6}$$

This last step might seem rather crude, but it will suffice for our purposes. Besides, Theorem 1 eventually establishes an equality considering Mattila's lower bound.

Utilising (5.5), we see that

$$\begin{split} \mathbb{E}_{\bar{\omega}_{n-k+1}^{1}} \sum_{\alpha=0}^{3} \left| \operatorname{proj} \mathcal{T}_{\alpha}^{k} (\bar{\omega}_{n-k+1}^{1}) \right| &= \frac{1}{4} \sum_{\alpha=0}^{3} \mathbb{E}_{\bar{\omega}_{n-k+2}^{1+\alpha}} \left| \operatorname{proj} \mathcal{D}_{k-1} (\bar{\omega}_{n-k+2}^{1+\alpha}) \right| \\ &= \frac{1}{4} (D_{k-1}^{1} + D_{k-1}^{2} + D_{k-1}^{3} + D_{k-1}^{4}) \\ &= D_{k-1}^{1}, \end{split}$$

since $D_{k-1}^{1+\alpha}=D_{k-1}^1$ for any $\alpha=0,1,2,3$. Applying this to (5.6), we get

$$D_k^1 \le D_{k-1}^1 - \mathbb{E}_{\bar{\omega}_{n-k+1}^1} \left| \operatorname{proj} \mathcal{T}_0^k (\bar{\omega}_{n-k+1}^1) \cap \operatorname{proj} \mathcal{T}_1^k (\bar{\omega}_{n-k+1}^1) \right|. \tag{5.7}$$

The final big step is to estimate the overlap term $|\operatorname{proj} \mathcal{T}_0^k(\bar{\omega}_{n-k+1}^1) \cap \operatorname{proj} \mathcal{T}_1^k(\bar{\omega}_{n-k+1}^1)|$ from below. But recall that $\mathcal{T}_0^k(\bar{\omega}_{n-k+1}^1)$ and $\mathcal{T}_1^k(\bar{\omega}_{n-k+1}^1)$ depend (aside from ω_{n-k+1}^1) respectively on $\bar{\omega}_{n-k+2}^1$ as in (5.4).

First, we average with respect to the subtrees $\bar{\omega}_{n-k+2}^1$ and $\bar{\omega}_{n-k+2}^2$, and afterwards we integrate over their common ancestor ω_{n-k+1}^1 . To simplify the notation, let us write $\bar{\omega}_{n-k+2}^{1,2}$ for both the subtrees $\bar{\omega}_{n-k+2}^1$ and $\bar{\omega}_{n-k+2}^2$. Then, we have

$$\begin{split} &\mathbb{E}_{\bar{\omega}_{n-k+2}^{1,2}} \left| \operatorname{proj} \mathcal{T}_{0}^{k} (\bar{\omega}_{n-k+1}^{1}) \cap \operatorname{proj} \mathcal{T}_{1}^{k} (\bar{\omega}_{n-k+1}^{1}) \right| \\ &= \mathbb{E}_{\bar{\omega}_{n-k+2}^{1,2}} \left| \operatorname{proj} \mathcal{T}_{0}^{k} (\omega_{n-k+1}^{1}, \bar{\omega}_{n-k+2}^{1}) \cap \operatorname{proj} \mathcal{T}_{1}^{k} (\omega_{n-k+1}^{1}, \bar{\omega}_{n-k+2}^{2}) \right| \\ &\stackrel{\underline{(5.1)}}{===} \int \mathbb{P}_{\bar{\omega}_{n-k+2}^{1,2}} \left(l^{\perp}(t) \cap \mathcal{T}_{0}^{k} (\omega_{n-k+1}^{1}, \bar{\omega}_{n-k+2}^{1}) \neq \emptyset \right. \\ & + \int \mathbb{P}_{\bar{\omega}_{n-k+2}^{1,2}} \left(l^{\perp}(t) \cap \mathcal{T}_{0}^{k} (\omega_{n-k+1}^{1}, \bar{\omega}_{n-k+2}^{1}) \neq \emptyset \right) \cdot \mathbb{P}_{\bar{\omega}_{n-k+2}^{1,2}} \left(l^{\perp}(t) \cap \mathcal{T}_{1}^{k} (\omega_{n-k+1}^{1}, \bar{\omega}_{n-k+2}^{2}) \neq \emptyset \right) dt \\ &= \int \mathbb{P}_{\bar{\omega}_{n-k+2}^{1}} \left(l^{\perp}(t) \cap \mathcal{T}_{0}^{k} (\omega_{n-k+1}^{1}, \bar{\omega}_{n-k+2}^{1}) \neq \emptyset \right) \cdot \mathbb{P}_{\bar{\omega}_{n-k+2}^{2}} \left(l^{\perp}(t) \cap \mathcal{T}_{1}^{k} (\omega_{n-k+1}^{1}, \bar{\omega}_{n-k+2}^{2}) \neq \emptyset \right) dt \\ &=: \mathcal{E}(\omega_{n-k+1}^{1}). \end{split}$$

The 3rd equality above holds because for a fixed angle ω_{n-k+1}^1 the events

$$\{l^{\perp}(t) \cap \mathcal{T}_{\alpha}^{k}(\omega_{n-k+1}^{1}, \bar{\omega}_{n-k+2}^{1+\alpha}) \neq \emptyset\}$$

for different α 's are independent.

It would be very nice if these two events would have the same probability for each t. Then, we would use Hölder's inequality to get that

$$\mathcal{E}(\omega_{n-k+1}^1) = \int \left[\mathbb{P}_{\bar{\omega}_{n-k+2}^1} \left(l^{\perp}(t) \cap \mathcal{T}_0^k(\omega_{n-k+1}^1, \bar{\omega}_{n-k+2}^1) \neq \emptyset \right) \right]^2 dt$$

$$\geq C \left(\int \mathbb{P}_{\bar{\omega}_{n-k+2}^1} \left(l^{\perp}(t) \cap \mathcal{T}_0^k(\omega_{n-k+1}^1, \bar{\omega}_{n-k+2}^1) \neq \emptyset \right) dt \right)^2.$$

Unfortunately, this is not the case.

Nevertheless, there is a way to approximate the overlap $\mathcal{E}(\omega_{n-k+1}^1)$. To keep things clean, let us denote

$$\psi := \omega_{n-k+1}^1, \ \bar{\psi}^1 := \bar{\omega}_{n-k+2}^1, \ \bar{\psi}^2 := \bar{\omega}_{n-k+2}^2 \quad \text{and} \quad s(\psi) := \frac{3}{4}(1 - \cos \psi),$$

and keep all angles fixed for now.

As discussed in Section 5.1, the average projections of $\mathcal{T}_0^k(\psi,\bar{\psi}^1)$ and $\mathcal{T}_1^k(\psi,\bar{\psi}^2)$ are shifted (and dilated) copies of $\mathcal{D}_{k-1}(\bar{\psi}^1)$ and $\mathcal{D}_{k-1}(\bar{\psi}^2)$, respectively. In particular, proj $\mathcal{T}_0^k(0,\bar{\psi}^1)$ and proj $\mathcal{T}_1^k(0,\bar{\psi}^1)$ are disjoint (cf (2.1) and (5.2)).

A simple geometric consideration (see Fig. 5) shows that the projections of $\mathcal{T}_0^k(0,\bar{\psi}^1)$ and $\mathcal{T}_0^k(\psi,\bar{\psi}^1)$ differ only by a shift of $s(\psi)$, i.e.

$$\operatorname{proj} \mathcal{T}_0^k(\psi, \bar{\psi}^1) = s(\psi) + \operatorname{proj} \mathcal{T}_0^k(0, \bar{\psi}^1).$$

Similarly, the projections of $\mathcal{T}_1^k(\psi, \bar{\psi}^2)$ and $\mathcal{T}_0^k(0, \bar{\psi}^1)$ differ (on average) by a shift of $s(\psi - \frac{\pi}{2})$. As a consequence, the events

$$\{l^{\perp}(t) \cap \mathcal{T}_0^k(\psi, \bar{\psi}^1) \neq \emptyset\}$$
 and $\{l^{\perp}(t) \cap \mathcal{T}_1^k(\psi, \bar{\psi}^2) \neq \emptyset\}$

might not have the same probability, but their probabilities are equal to

$$\mathbb{P}_{\bar{\psi}^1}\left(l^{\perp}(t')\cap\mathcal{T}_0^k(0,\bar{\psi}^1)\right)$$

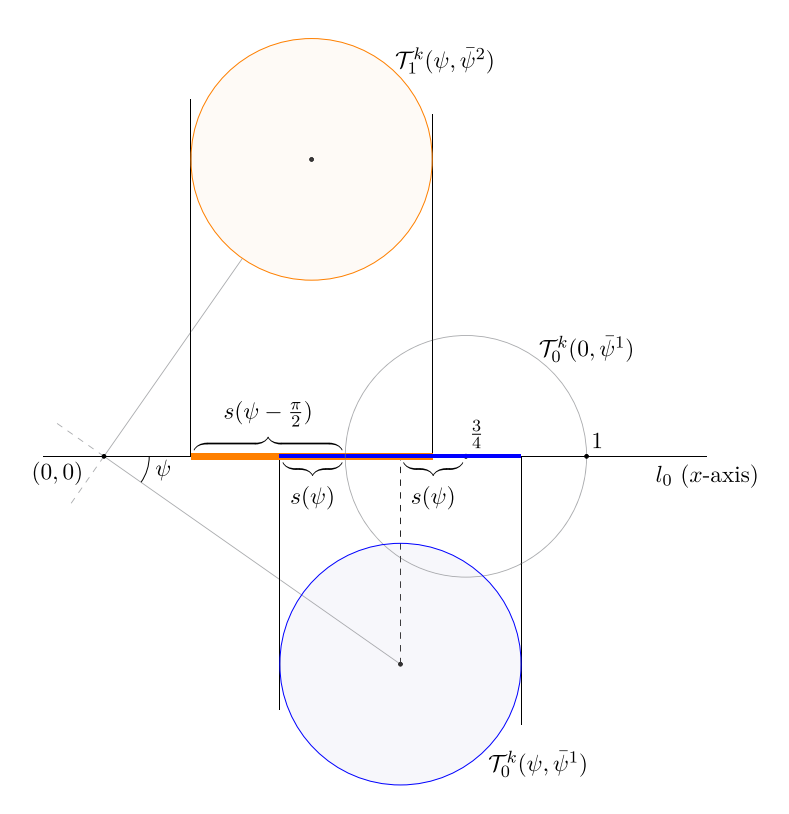


Fig. 5. The projections of $\mathcal{T}_0^k(\psi,\bar{\psi})$ and $\mathcal{T}_1^k(\psi,\bar{\psi})$ are contained in copies of the interval $(\frac{1}{2},1)$ shifted by $s(\psi)$ and $s(\psi-\frac{\pi}{2})$, respectively.

for some appropriately shifted t', since $\bar{\psi}^1$ and $\bar{\psi}^2$ are independent. We make this explicit in the following lemma.

Lemma 3. With notation as above, it holds that

$$\mathbb{P}_{\bar{\psi}^1}\left(l^\perp(t)\cap\mathcal{T}^k_0(\psi,\bar{\psi}^1)\neq\emptyset\right)=\mathbb{P}_{\bar{\psi}^1}\left(l^\perp(t+s(\psi))\cap\mathcal{T}^k_0(0,\bar{\psi}^1)\neq\emptyset\right)$$

and

$$\mathbb{P}_{\bar{\psi}^2}\left(l^{\perp}(t)\cap\mathcal{T}_1^k(\psi,\bar{\psi}^2)\neq\emptyset\right) = \mathbb{P}_{\bar{\psi}^1}\left(l^{\perp}(t+s(\psi-\frac{\pi}{2}))\cap\mathcal{T}_0^k(0,\bar{\psi}^1)\neq\emptyset\right). \tag{5.8}$$

With Lemma 3 at hand along with (5.1), we can rewrite the overlap with our current notation in a more convenient way. First, let us denote

$$F(t) := \mathbb{P}_{\bar{\psi}^1} \left(l^{\perp}(t) \cap \mathcal{T}_0^k(0, \bar{\psi}^1) \right). \tag{5.9}$$

Then, we see that

$$\begin{split} \mathcal{E}(\psi) &= \int \mathbb{P}_{\bar{\psi}^1} \left(l^\perp(t) \cap \mathcal{T}_0^k(\psi, \bar{\psi}^1) \neq \emptyset \right) \cdot \mathbb{P}_{\bar{\psi}^2} \left(l^\perp(t) \cap \mathcal{T}_1^k(\psi, \bar{\psi}^2) \neq \emptyset \right) dt \\ &= \int \mathbb{P}_{\bar{\psi}^1} \left(l^\perp(t + s(\psi)) \cap \mathcal{T}_0^k(0, \bar{\psi}^1) \neq \emptyset \right) \cdot \mathbb{P}_{\bar{\psi}^1} \left(l^\perp(t + s(\psi - \frac{\pi}{2})) \cap \mathcal{T}_0^k(0, \bar{\psi}^1) \neq \emptyset \right) dt \\ &= \int F(t + s(\psi)) \cdot F(t + s(\psi - \frac{\pi}{2})) dt, \end{split}$$

where the first equality is simply the definition of \mathcal{E} .

At this point, if we integrate over $\psi \in [0, \frac{\pi}{2}]$, we get that the

Expectation of the overlap =
$$\int \mathcal{E}(\psi)d\psi = \int \int F(t+s(\psi)) \cdot F(t+s(\psi-\frac{\pi}{2}))d\psi dt.$$

Let's make this change of variables: $u = t + \frac{3}{4}(1 - \cos\psi)$ and $v = t + \frac{3}{4}(1 - \cos(\psi - \frac{\pi}{2}))$. The Jacobian of this change is at most $\frac{3\sqrt{2}}{4}$, and thus

Expectation of the overlap
$$\geq \frac{4}{3\sqrt{2}} \int \int F(u)F(v)dudv = \frac{2\sqrt{2}}{3} \left(\int F(t)dt \right)^2$$
.

Now, we can revert to our initial notation. And since there is no dependence on $\bar{\omega}_{n-k+1}^3$ or $\bar{\omega}_{n-k+1}^4$, we get

$$\begin{split} \mathbb{E}_{\bar{\omega}_{n-k+1}^{1}} \left| \operatorname{proj} \mathcal{T}_{0}^{k} (\bar{\omega}_{n-k+1}^{1}) \cap \operatorname{proj} \mathcal{T}_{1}^{k} (\bar{\omega}_{n-k+1}^{1}) \right| \\ &= \operatorname{Expectation of the overlap} \\ &\geq \frac{2\sqrt{2}}{3} \left(\mathbb{E}_{\bar{\omega}_{n-k+1}^{1}} \left| \operatorname{proj} \mathcal{T}_{0}^{k} (\bar{\omega}_{n-k+1}^{1}) \right| \right)^{2} \\ &= \frac{(5.5)}{3} \cdot \frac{2\sqrt{2}}{3} \cdot \frac{1}{16} \left(\mathbb{E}_{\bar{\omega}_{n-k+2}^{1}} \left| \operatorname{proj} \mathcal{D}_{k-1} (\bar{\omega}_{n-k+2}^{1}) \right| \right)^{2} \\ &= \frac{1}{12\sqrt{2}} (D_{k-1}^{1})^{2}. \end{split}$$

Finally, combining the fact that

$$\mathbb{E}_{\bar{\omega}_{n-k+1}^1} \left| \text{proj } \mathcal{T}_0^k(\bar{\omega}_{n-k+1}^1) \cap \text{proj } \mathcal{T}_1^k(\bar{\omega}_{n-k+1}^1) \right| \ge \frac{1}{12\sqrt{2}} (D_{k-1}^1)^2$$

with (5.7) and setting $c = 12\sqrt{2}$ we get

$$D_k^1 \le D_{k-1}^1 - c^{-1}(D_{k-1}^1)^2.$$

Lemma 2 is proved.

6. Comparison with [12] and [11]

The random Cantor set in [12] is a very close relative of the random Cantor set in this note, the difference is that Zhang's random construction of n generations has n independent rotations involved, whereas our construction has $1 + \cdots + 4^{n-1}$ independent rotations. There the disks of generation k are rotated by the same angle ω_k , while in this note we have 4^{k-1} independent rotations of disks of generation k. Naturally, it is more difficult to work in a more chaotic model such as ours, and the techniques here use independence in a more involved way than in [12]. It is just a little harder to make sense of the combinatorics involved in our model.

On the other hand, there are many "common places": the use of overlap as the way to see the rate of decays of successive approximations of the random Cantor set, the use of Lemma 2, as well as the technical Lemma 3.

Concerning [11], there are two main differences which create difficulties. The first is the fact that at most two of the projections $\operatorname{proj}_{\theta} \mathcal{T}_{\alpha}^{k}(\bar{\omega}_{n-k+1}^{1})$ can intersect at each point on the line l_{θ} . This is equivalent to

line $l_{\theta}^{\perp}(t)$ intersecting at most two of the disks for any t, and is key to the square factor appearing in our calculations.

However, this is simply not true in the case of squares. In fact, in the Peres and Solomyak case the corresponding line $l_{\theta}^{\perp}(t)$ can simultaneously intersect 3 squares of generation k for any k and any t. Because of this, the inequalities appearing here cannot be translated directly in the square setting.

But even if this wasn't an obstacle, the reader should pay attention to Lemma 3. Let's pretend that we can repeat everything before this lemma for the model of Peres and Solomyak. The role of the angle ω_{n-k+1}^1 will be played by the "Favard angle" θ , the shift function $s(\omega_{n-k+1}^1)$ will be replaced by

$$s(\theta) = \frac{1}{2}\sin\theta,$$

and all seems to be following smoothly along the same lines. Also, the following equality

$$\int \mathbb{E}\mathbf{1}_{\left\{l_{\theta}^{\perp}(t)\cap\mathcal{T}_{0}^{k}(\bar{\omega}_{n-k+1}^{1})\neq\emptyset\right\}}d\theta = \int \mathbb{E}\mathbf{1}_{\left\{l_{\theta}^{\perp}(t+s(\theta))\cap\mathcal{T}_{1}^{k}(\bar{\omega}_{n-k+1}^{1})\neq\emptyset\right\}}d\theta,\tag{6.1}$$

which would be the analogue of (5.8), makes sense in principle if we understand ω 's as the random variables in the Peres–Solomyak model, which assume the values 0, 1, 2, 3 (instead of values in the interval $[0, \frac{\pi}{2}]$ as in our's and Zhang's models).

But, there is a caveat. We reduced the function of two variables

$$G(\psi,t) := \mathbb{P}_{\bar{\omega}_{n-k+2}^1} \left(l^{\perp}(t) \cap \mathcal{T}_0^k(\psi,\bar{\omega}_{n-k+2}^1) \neq \emptyset \right)$$

to the composition with a function of one variable and the shift (see (5.9) for the definition of F):

$$G(\psi, t) = G(0, t + s(\psi)) = F(t + s(\psi))$$
 (6.2)

thanks to (5.8). But looking at (6.1), we can notice that the function

$$\mathcal{G}(\theta,t) := \mathbb{E} \mathbf{1}_{\left\{l_{\theta}^{\perp}(t) \cap \mathcal{T}_{0}^{k}(\bar{\omega}_{n-k+2}^{1}) \neq \emptyset\right\}}$$

cannot be written as some $\mathcal{F}(t+S(\theta))$.

As a result of this misfortune, we cannot write

Expectation of the overlap =
$$\int \mathcal{E}(\theta)d\theta = \int \int \mathcal{F}(t+S(\theta)) \cdot \mathcal{F}(t)d\theta dt$$

as before. Working similarly, this would in turn bring about the term $(\int \mathcal{F}dt)^2$. Instead, we only have that

Expectation of the overlap =
$$\int \mathcal{E}(\theta)d\theta = \int \int \mathcal{G}(\theta,t) \cdot \mathcal{G}(\theta,t+S(\theta)))d\theta dt$$
,

and it is not clear (at least to us) how to estimate this integral from below as no change of variables seems to be of help.

Acknowledgments

We are grateful to the referee for their valuable feedback and comments.

References

- [1] M. Bateman, A. Volberg, An estimate from below for the Buffon needle probability of the four-corner Cantor set, Math. Res. Lett. 17 (5) (2010) 959–967, https://doi.org/10.4310/mrl.2010.v17.n5.a12.
- [2] M. Bond, I. Łaba, A. Volberg, Buffon's needle estimates for rational product Cantor sets, Am. J. Math. 136 (2) (2014) 357–391, https://doi.org/10.1353/ajm.2014.0013.
- [3] M. Bond, A. Volberg, Buffon needle lands in ϵ -neighborhood of a 1-dimensional Sierpinski Gasket with probability at most $|\log \epsilon|^{-c}$, C. R. Math. 348 (11–12) (June 2010) 653–656, https://doi.org/10.1016/j.crma.2010.04.006.
- [4] M. Bond, A. Volberg, Buffon's needle landing near Besicovitch irregular self-similar sets, Indiana Univ. Math. J. 61 (6) (2012) 2085-2109, https://doi.org/10.1512/jumj.2012.61.4828.
- [5] I. Laba, Recent progress on Favard length estimates for planar Cantor sets, in: Operator-Related Function Theory and Time-Frequency Analysis, Springer International Publishing, Sept. 2014, pp. 117–145.
- [6] I. Łaba, K. Zhai, The Favard length of product Cantor sets, Bull. Lond. Math. Soc. 42 (6) (Aug. 2010) 997–1009, https://doi.org/10.1112/blms/bdq059.
- [7] P. Mattila, Hausdorff dimension, projections, and the Fourier transform, Publ. Mat. 48 (Jan. 2004) 3–48, https://doi.org/10.5565/publmat_48104_01.
- [8] P. Mattila, Fourier Analysis and Hausdorff Dimension, Cambridge University Press, 2015.
- [9] P. Mattila, Hausdorff dimension, orthogonal projections and intersections with planes, Ann. Acad. Sci. Fenn., Ser. A I Math. 1 (1975) 227–244, https://doi.org/10.5186/aasfm.1975.0110.
- [10] F. Nazarov, Y. Peres, A. Volberg, The power law for the Buffon needle probability of the four-corner Cantor set, St. Petersburg Math. J. 22 (1) (Feb. 2011) 61, https://doi.org/10.1090/s1061-0022-2010-01133-6.
- [11] Y. Peres, B. Solomyak, How likely is Buffon's needle to fall near a planar Cantor set?, Pac. J. Math. 204 (2) (June 2002) 473–496, https://doi.org/10.2140/pjm.2002.204.473.
- [12] S. Zhang, The exact power law for Buffon's needle landing near some random Cantor sets, Rev. Mat. Iberoam. 36 (2) (Dec. 2019) 537–548, https://doi.org/10.4171/rmi/1138.

Further reading

- [13] T. Tao, A quantitative version of the Besicovitch projection theorem via multiscale analysis, Proc. Lond. Math. Soc. 98 (3) (Oct. 2008) 559–584, https://doi.org/10.1112/plms/pdn037.
- [14] X. Tolsa, Analytic capacity, rectifiability, and the Cauchy integral, in: Proceedings of the International Congress of Mathematicians, Madrid, August 22–30, European Mathematical Society Publishing House, 2006, pp. 1505–1527.